BIOLOGY OF REPRODUCTION **66,** 866–876 (2002)

Subcellular Distribution of ZP1, ZP2, and ZP3 Glycoproteins During Folliculogenesis and Demonstration of Their Topographical Disposition Within the Zona Matrix of Mouse Ovarian Oocytes[1]

Majid El-Mestrah,[3] Philip E. Castle,[4] Girum Borossa,[3] and Frederick W.K. Kan[2,3]

Department of Anatomy and Cell Biology,[3] Faculty of Health Sciences, Queen's University, Kingston, Ontario, Canada K7L 3N6
Laboratory of Cellular and Developmental Biology,[4] National Institutes of Diabetes and Digestive and Kidney Diseases, National Institutes of Health, Bethesda, Maryland 20892

ABSTRACT

The zona pellucida (ZP) is an extracellular coat synthesized and secreted by the oocyte during follicular development and surrounding the plasma membrane of mammalian eggs. To date, the mechanism of synthesis and secretion, mode of assembly, and intracellular trafficking of the ZP glycoproteins have not been fully elucidated. Using antibodies against mouse ZP1, ZP2, and ZP3 in conjunction with the protein A-gold technique, we have shown an association of immunolabeling with the Golgi apparatus, secretory granules, and a complex structure called vesicular aggregate, respectively, in mouse ovarian follicles. In contrast, the neighboring granulosa cells were not reactive to any of the three antibodies used. Immunolabeling of ZP1, ZP2, and ZP3 was detected throughout the entire thickness of the ZP, irrespective of the developmental stage of ovarian follicles. Double and triple immunolocalization studies, using antibodies tagged directly to different sizes of gold particles, revealed an asymmetric spatial distribution of the three ZP glycoproteins in the zona matrix at various stages of follicular development. All three glycoproteins were specifically localized over small patches of darkly stained flocculent substance dispersed throughout the zona matrix. Very often, ZP1, ZP2, and ZP3 were found in close association. These results confirm findings from previous studies demonstrating that ovarian oocytes and not granulosa cells are the only source for mouse ZP glycoproteins. In addition, results from our morphological and immunocytochemical experiments suggest that the vesicular aggregates in the ooplasm are likely to serve as an intermediary in the synthesis and secretion of ZP glycoproteins. The stoichiometric disposition of ZP1, ZP2, and ZP3 in the zona matrix as revealed by double and triple immunolocalization studies provide further insight into some of the unanswered questions pertinent to the current model of mouse ZP structure proposed by the Wassarman group.

female reproductive tract, fertilization, follicle, oocyte development, ovary

INTRODUCTION

The zona pellucida (ZP) is a thick extracellular coat that surrounds growing oocytes, ovulated eggs, and preimplantation embryos in mammals [1]. The ZP contains receptors that mediate initial interactions between the sperm and egg as a prelude to fertilization; it also mediates the relative species-specificity during gamete interaction, prevents polyspermy, and protects the developing embryo prior to implantation [1, 2].

The origin of the ZP glycoproteins has been a matter of controversy for some time. Both the oocyte and/or the surrounding granulosa cells have been proposed to be the origin of the ZP glycoproteins [3–9]. However, in mice (the most well-studied system) the site of synthesis and secretion of the major ZP glycoproteins (ZP1, ZP2, and ZP3) has been associated exclusively with the growing oocyte itself and not with the surrounding follicular cells [3, 10–12]. In this regard, the biosynthetic pathways for mouse ZP1, ZP2, and ZP3 have been suggested to resemble those described for other glycoproteins secreted by eukaryotic cells [13]; however, the exact mechanism of their synthesis and secretion at the subcellular level and their intracellular trafficking remain to be fully elucidated. Also, whether the ZP is structurally homogeneous throughout its thickness continues to be the subject of some disagreement [14, 15]. Structurally, the three sulfated glycoproteins, ZP1, ZP2, and ZP3, assemble to form a three-dimensional matrix. A model for ZP structure is derived from the conjunctive application of ultrastructural observations [16, 17], which strongly suggests a meshwork of well-knitted filamentous structure for the ZP, and quantification of ZP1, ZP2, and ZP3 by gel densitometry [17, 18]. As such, the mouse ZP is an extensive three-dimensional array of long interconnected filaments that consist of a structural repeat. The filaments are constructed by alternating molecules of ZP2 and ZP3, randomly cross-linked by ZP1 through intermolecular disulfide bonds [17]. Although the current model of the arrangement and spatial distribution of mouse ZP as proposed by Wassarman and Mortillo [17] is consistent with experimental observations, formal proof that the ZP is constructed in this way is still lacking. In the hope of shedding some light on the structure and assembly of the mouse zona pellucida, we employed specific antibodies against each of ZP1, ZP2, and ZP3 to examine at the electron microscope level the subcellular distribution of mouse ZP glycoproteins in the oocyte proper during follicular development in the ovary. We also used the double and triple immunolocalization approach to examine the spatial topography of the three ZP glycoproteins in the zona matrix of mouse ovarian oocytes.

MATERIALS AND METHODS

Preparation of Ovarian Tissue

Twelve sexually mature (3–4 wk old) female CD1 mice (Charles River, St-Constant, PQ, Canada) were killed by cervical dislocation. Their ovaries were excised, washed briefly with PBS (pH 7.4), and immediately fixed for 2 h at 4°C by immersion in 2.5% glutaraldehyde in 0.1 M sodium cacodylate buffer (pH 7.4). For immunocytochemical labeling at the light and electron microscope levels, ovarian tissue samples were processed and

[1]This study was supported by the Canadian Institutes of Health Research.
[2]Correspondence. FAX: 613 533 2566; e-mail: kanfwk@post.queensu.ca

Received: 23 May 2001.
First decision: 7 June 2001.
Accepted: 25 October 2001.
© 2002 by the Society for the Study of Reproduction, Inc.
ISSN: 0006-3363. http://www.biolreprod.org

embedded in paraffin and Lowicryl K4M (CANEMCO, St. Laurent, PQ, Canada), respectively, according to routine procedures. Some ovarian tissue samples designated for morphological study were either postfixed with 1% osmium tetroxide (CANEMCO) in nanopure water for 2 h at 4°C or treated with ferrocyanide-reduced osmium tetroxide [19], dehydrated in a series of graded ethanol solutions, infiltrated, and embedded in Epon 812 according to routine procedures.

Antibodies

The two sets of specific antibodies used in this study were generously provided by Dr. Jurrien Dean (Laboratory of Cellular and Developmental Biology, National Institutes of Diabetes and Digestive and Kidney Diseases, National Institutes of Health, Bethesda, MD). The first set consisted of monoclonal antibodies M-1.4 (rat IgG), IE-3 (rat IgG), and IE-10 (rat IgG), which are specific for mouse ZP1, ZP2, and ZP3, respectively. The second set of monoclonal antibodies included anti-ZP1, anti-ZP2, and anti-ZP3 antibodies that were directly bound to colloidal gold particles with a diameter of 10 or 15 nm, 5 or 15 nm, and 5 or 10 nm, respectively, as per the instructions of the manufacturer of the colloidal gold (BBInternational, Cardiff, U.K.). The specificity of each of the three monoclonal antibodies has been previously demonstrated [20–22].

Immunocytochemistry

All labeling procedures were carried out at room temperature. For immunoelectron microscopy, thin sections of Lowicryl-embedded ovarian tissue samples were first incubated for 10 min on a drop of PBS (0.01 M) containing 1% BSA followed by a 1-h incubation on a drop of one of the monoclonal anti-ZP1, anti-ZP2, or anti-ZP3 antibodies diluted in PBS. After three washes of 5 min each in PBS, ovarian sections were incubated for 1 h with rabbit anti-rat IgG polyclonal antibody diluted in PBS. Tissue sections were rinsed with PBS, transferred onto a drop of PBS containing 1% BSA, and incubated for 30 min with protein A-gold complex. Colloidal gold particles 15 nm in diameter were used. Thin sections of Lowicryl-embedded ovaries designated for double or triple immunolocalization studies were initially incubated with 1% ovalbumin in PBS for 10 min, labeled for 1 h with either a single antibody-gold conjugate solution or a combination of two or three different antibody-gold conjugates mixed in equal volumes for 1 h prior to use. After being labeled, tissue sections were washed with PBS and distilled water. All labeled sections were counterstained with uranyl acetate and lead citrate before being examined on a Hitachi 7000 electron microscope operated at 75 kV.

Immunocytochemical Controls

To establish the specificity of the immunolabeling, the following immunocytochemical controls were used: 1) substitution of the primary or secondary antibody with the corresponding buffer, 2) substitution of the antibody-gold conjugates with the protein A-gold complex alone, or 3) substitution of the primary antibody with a monoclonal antibody directed against hamster oviductin, a glycoprotein expressed exclusively in the oviduct and not in other tissues [23].

RESULTS

Ultrastructural Morphology of the Secretory Apparatus in the Oocyte Proper and the ZP of Fully Grown Ovarian Oocytes

Electron microscopic examination of multilayered ovarian follicles showed the presence of a complex secretory machinery in the oocyte proper distinctive to fully grown oocytes. Round and oval-shaped mitochondria were abundant and were closely associated with isolated cisternae of smooth endoplasmic reticulum (Fig. 1). The abundance of ribosomes in small clusters and the accumulation of stacks of annulate lamellae throughout the oocyte proper were prominent features (Fig. 1a). Well-preserved and favorably cut sections of the oocyte revealed some of the structural details of the filamentous network that makes up the ZP. In particular, the outer ZP showed linear arrays of filamentous materials that ran parallel to the surface of the oolemma (Fig. 1a). Unlike when osmium tetroxide was used alone, in tissue sections prepared from ovarian tissue postfixed with ferrocyanide-reduced osmium tetroxide the membranous features and structural details of various cellular organelles and the ZP were further enhanced (Fig. 1, a and b). The bulk of various large membrane-bound vesicles and their associated smaller vesicles, which constitute the vesicular aggregate, presented overall well-defined ultrastructural features. Clusters of ribosomes dispersed throughout the oocyte proper displayed a higher intensity of staining (Fig. 1a) and the presence of two different types of cortical granules based on their distinct staining properties was also well demonstrated (Fig. 1a). A well-developed Golgi complex with an elaborate organization was evident especially at the late stages of oocyte growth (data not shown). The most conspicuous characteristic of the oocyte proper, however, was the presence of a number of vesicular aggregates, mostly in the vicinity of the oolemma (Fig. 1a). A close examination of a vesicular aggregate revealed its distinctive appearance in the form of a complex of membrane-bound vesicles of various sizes (Fig. 1b). Each vesicular aggregate complex consisted of four or more large membranous vesicles embedded in a mass of smaller smooth vesicles relatively uniform in size. These large membrane-bound vesicles were filled with an amorphous substance and surrounded concentrically by a layer of small vesicles of uniform size (Fig. 1b). On many occasions, the large membrane-bound vesicles were found in isolation throughout the oocyte proper of fully grown oocytes.

Immunolabeling for ZP1, ZP2, and ZP3 in the ZP and the Oocyte Proper

When thin sections of Lowicryl-embedded ovarian tissue were labeled with anti-ZP1 antibody followed by secondary antibody-protein A-gold complex, the ZP of ovarian oocytes was uniformly labeled irrespective of the stage of follicular development. In early unilaminar primary follicles, labeling of the ZP was concentrated in pockets between the oocyte surface and cytoplasmic processes of the surrounding follicular cells (Fig. 2a). An increase in the intensity of labeling by gold particles was noted in parallel with the increase in diameter of growing oocytes (Fig. 2b). When the oocyte proper of ovarian tissue sections was incubated with the anti-ZP1 antibody, immunolabeling of moderate intensity was revealed over the Golgi complex (Fig. 2c), secretory granules, and the vesicular aggregate. Similar results were achieved when ovarian sections were labeled with antibody against ZP2 or ZP3 followed by secondary antibody-protein A-gold complex (results not shown). In tissue sections incubated with either anti-ZP2 (not shown) or anti-ZP3 antibody (Fig. 3, a and b), labeling by gold particles was associated with the linear arrays of filaments, which run tangentially in the outer region of the zona matrix. Overall, distribution of gold particles over the ZP resulting from incubations of ovarian tissue sections with anti-ZP3, anti-ZP2, and anti-ZP1 antibodies indicated that ZP3 consistently had the highest intensity of labeling. Granulosa cells surrounding the oocyte were not reactive to anti-ZP1, anti-ZP2, or anti-ZP3 antibody (Figs. 2b and 3a). Control sections incubated with protein A-gold complex alone or labeled with a monoclonal antibody directed against hamster oviductin showed a negative reaction over the different subcellular structures and ZP, demonstrating the specificity of the labelings (Fig. 3c).

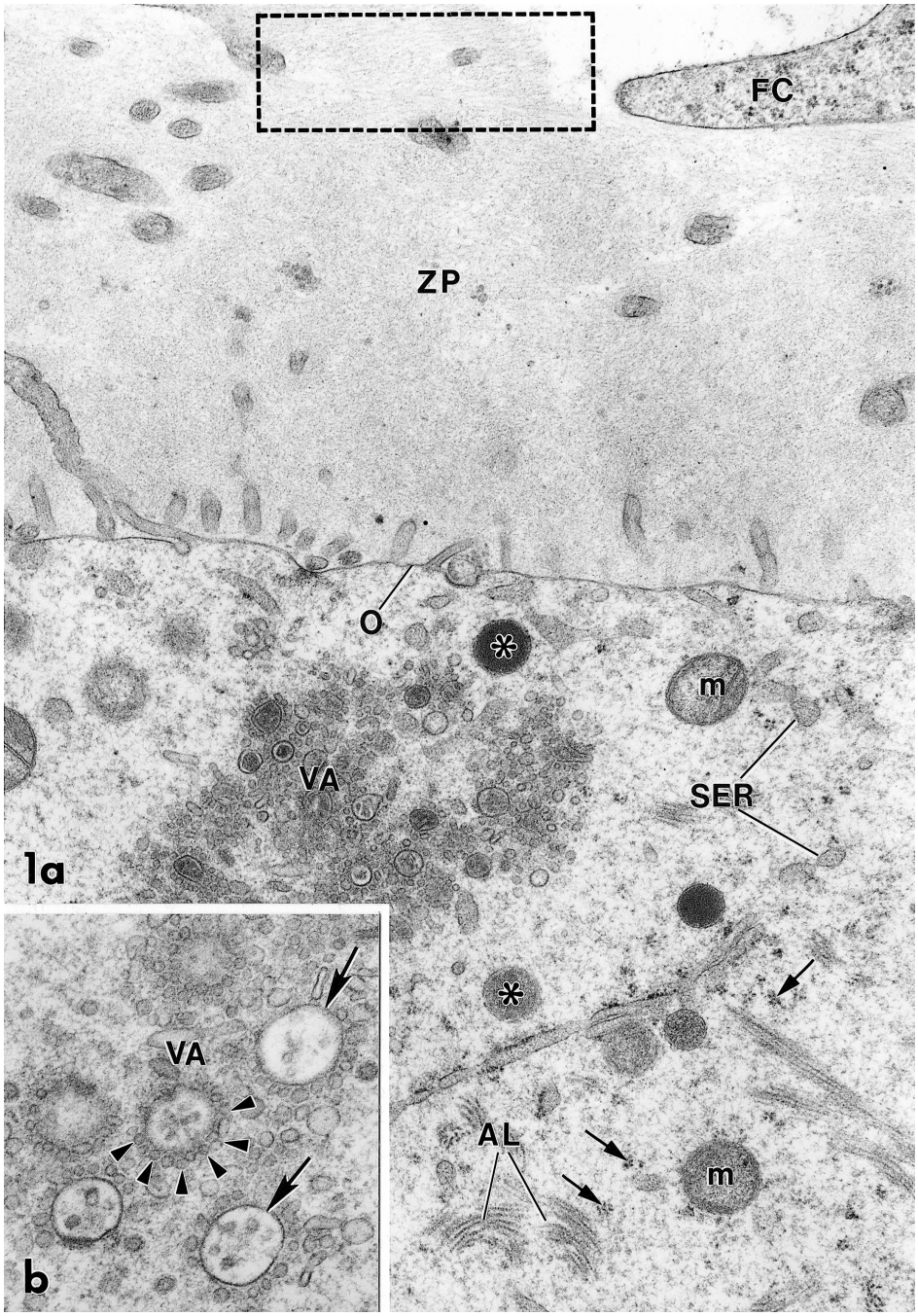

FIG. 1. Electron micrograph of Epon-embedded thin section of mouse ovarian multilaminar secondary follicle postfixed with ferrocyanide-reduced osmium tetroxide showing the presence of a vesicular aggregate (VA) below the oolemma (O), clusters of ribosomes (arrows), and cortical granules (asterisks) of differential staining properties (**a**). In the outer layer of the ZP (framed box), the filaments run in a horizontal plane parallel to the surface of the oocyte. A higher magnification electron photomicrograph (**b**) reveals the structural details of a VA made up of several large membranous vesicles (arrows), each of which is surrounded by a layer of small vesicles. m, Mitichondria; AL, annulate lamellae; FC, follicular cell; SER, smooth endoplasmic reticulum. **a**, ×30 000; **b**, ×46 000.

Topographical Distribution of ZP1, ZP2, and ZP3 in the Zona Matrix

When thin sections of Lowicryl-embedded ovaries were incubated with each of the three anti-ZP antibodies conjugated directly to gold particles, several patterns of immunolabeling were observed. In immunolabeling experiments carried out with all anti-ZP antibody-gold conjugates, colloidal gold particles were asymmetrically distributed in the zona matrix of ovarian follicles in various developmental stages with a higher concentration of gold labeling observed in the inner region of the ZP. This asymmetric distribution was most prominent when anti-ZP1 antibody-gold conjugate (15 nm in diameter) was used (Fig. 4a). Within the zona matrix, gold particles were associated with linearly arranged filaments (Fig. 4a). In the oocyte proper, the vesicular aggregate was also strongly labeled by gold particles (Fig. 4b), similar to the labeling observed with the different unconjugated rat IgG anibodies.

The main objective of using different anti-ZP antibodies conjugated directly to different sizes of gold particles was to examine the spatial relationship and topographical disposition of ZP1, ZP2, and ZP3 in the zona matrix. Immunogold labeling experiments using a combination of two antibodies (ZP1 and ZP2 or ZP1 and ZP3) demonstrated an interesting pattern of colloidal gold distribution. At low magnification, a homogeneous distribution of the 10-nm and 5-nm gold particles, representing ZP1 and ZP3, respectively, was seen over the entire ZP (Fig. 5a). For the most part, there seemed to be an aggregation of immunolabeling by gold particles representing both anti-ZP1 and anti-ZP3 antibodies (10 nm and 5 nm, respectively; Fig. 5, a and b). The immunolabeling for ZP1 appeared to be more

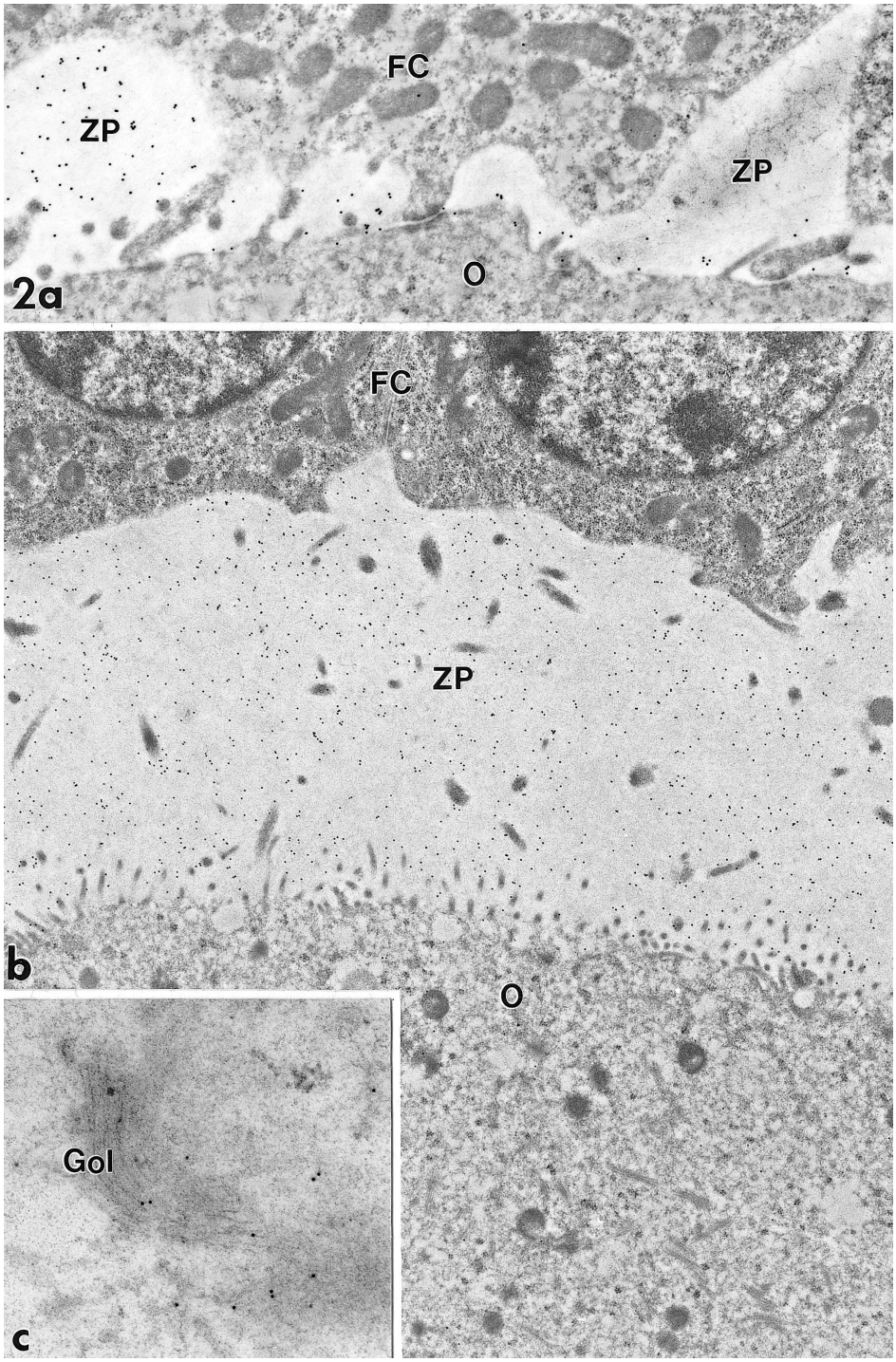

FIG. 2. Lowicryl thin sections of ovarian oocytes at various stages of follicular development incubated with anti-ZP1 antibody/rabbit anti-rat IgG/protein A-gold complex. Pockets of newly synthesized ZP located between the follicular cells and oocyte (O) of a unilaminar primary follicle show relatively moderate labeling by gold particles (**a**). Immunolabeling of high intensity is visible throughout the entire thickness of the ZP of a multilaminar follicle (**b**). Follicular cells (FC) are devoid of any labeling (**b**), whereas the Golgi apparatus (Gol) in the oocyte proper of a multilaminar follicle displays a heavy reaction to anti-ZP1 antibody (**c**). **a**, ×25 000; **b**, ×41 500; **c**, ×60 000.

intense than that for ZP3. Many of the 10-nm gold particles (representing ZP1) were <10 nm apart (Fig. 5b). The close association between two sizes of gold particles was not evident, however, when the anti-ZP1 antibody-gold conjugate was used in combination with the anti-ZP2 antibody-gold conjugate. Thin sections of Lowicryl-embedded ovaries were labeled with a combination of all three antibody-gold conjugate solutions directed, respectively, against ZP1, ZP2, and ZP3, and examined with an electron microscope. At low magnification (Fig. 6a), there was no apparent direct association between the different sizes of colloidal gold particles that represent the three different ZP glycoproteins. Labeling by the three antibodies occupied the entire ZP, with a relatively high concentration of gold particles detected in the inner layer of the zona matrix. However, a close examination of the pattern of labeling over the zona matrix at high magnifications showed the distribution of gold particles of various sizes more often in clusters or in linear arrays of one particular gold size (Figs. 6b and 7). Immunogold labeling (15-nm particle size) for ZP1 appeared to yield the highest labeling intensity and was specifically confined to small darkly stained patches of filamentous meshwork with a distance of less than 10 nm separating many of the 15-nm gold particles (Figs. 6b and 7). Labeling for ZP2 (5-nm particle size), when present, was often seen in close association with immunogold particles

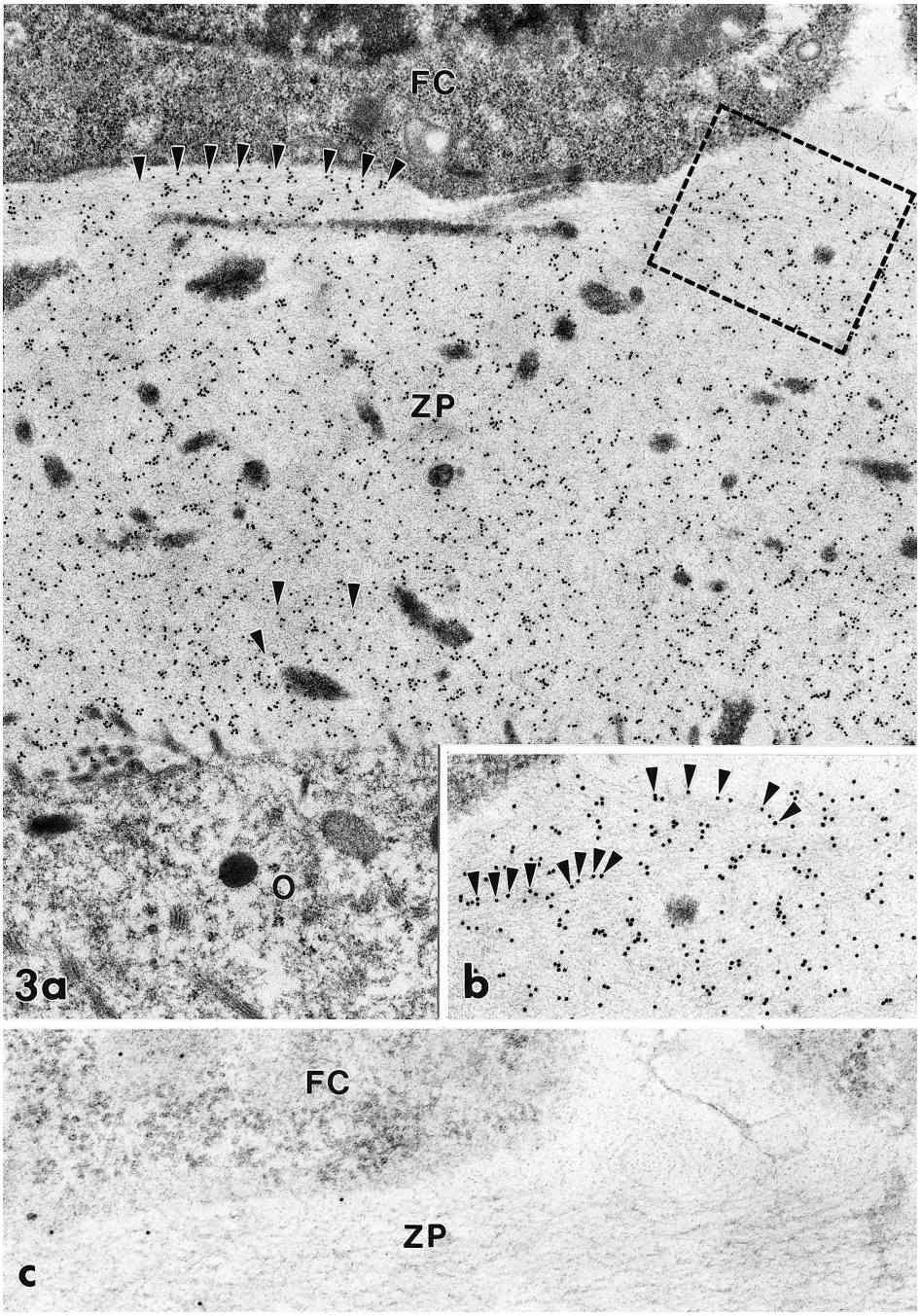

FIG. 3. Electron micrographs of a multilaminar secondary follicle labeled with anti-ZP3/rabbit anti-rat IgG/protein A-gold (**a** and **b**) or with a monoclonal antibody directed against hamster oviductin (**c**). **a**) The ZP shows labeling by gold particles of filaments located in the outer region of the zona matrix (arrowheads). Follicular cells (FC) are devoid of any labeling by anti-ZP3 antibody. ×21 000. **b**) Higher magnification of the framed box (**a**) showing the gold particles (arrowheads) directly superimposed on the linear arrays of filaments. ×58 000. **c**) In high magnification view of a control section, the horizontal arrays of filaments in the ZP are devoid of gold particles. ×60 000.

(10 nm) specific for ZP3 (Fig. 7). On many occasions, 5-nm (ZP2) and 10-nm (ZP3) gold particles were observed at the periphery of patches of darkly stained material decorated with 15-nm gold particles (ZP1; Fig. 7). The network of lightly stained thinner filaments interconnecting the darkly stained patches was not reactive to any of the three antibodies. Overall, when a combination of two or three antibody-gold solutions was used, the distribution and pattern of labeling in the zona matrix were similar to those observed in thin sections labeled with a single antibody-gold conjugate solution. Control ovarian sections incubated with the protein A-gold complex alone instead of the different antibody-gold conjugates showed an absence of gold particles in the oocyte proper and ZP, demonstrating the specificity of these labelings.

DISCUSSION

With the hope of elucidating the subcellular distribution of the major ZP glycoproteins and their spatial relationships in the zona matrix of mouse ovarian oocytes, ultrastructural, cytochemical, and immunogold colocalization experiments were carried out utilizing antibodies specific for ZP1, ZP2, and ZP3. General morphological features of mouse ovarian oocytes during the early and late stages of follicular development have been previously reviewed [24]. Besides the usual organelles found in the oocyte proper, the existence of a complex structure, the vesicular aggregate, has been documented in mouse and human ovarian oocytes [25–28]. Ultrastructural features of this vesicular aggregate, however, have not been well characterized, and information

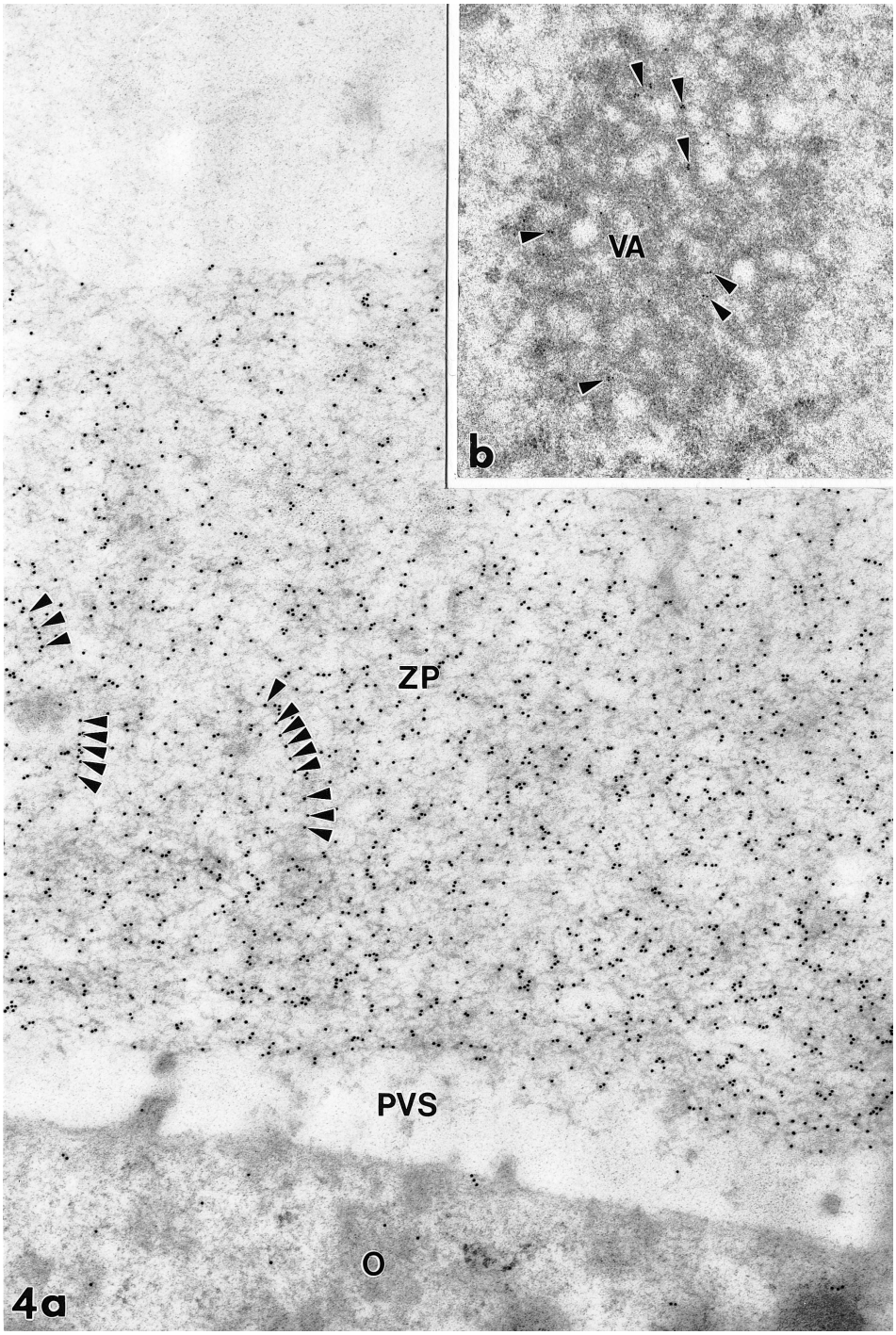

FIG. 4. Lowicryl section showing a multilaminar secondary follicle immunolabeled with anti-ZP1 antibody directly conjugated to 15-nm gold particle. **a**) Immunolabeling (arrowheads) for ZP1 is confined to linear arrays of filaments, with the disposition of gold particles at more or less regular intervals along the filaments. ×51 000. **b**) In the oocyte proper, a vesicular aggregate (VA) complex is strongly labeled by gold particles (arrowheads). ×30 000. O, Oocyte; PVS, perivitelline space.

about the role of this complex structure in the ovarian oocyte is also lacking. Recently, we reported the localization of various lectin-binding sites in the vesicular aggregates in the mouse ovarian oocytes during folliculogenesis [29]. In the present study, the localization of ZP1, ZP2, and ZP3 over the Golgi complex, secretory granules, and the vesicular aggregate and its isolated membrane-bound structures is suggestive of active involvement of these subcellular organelles in processing the three glycoproteins before they are secreted to form the ZP. In particular, the present finding of the localization of ZP1, ZP2, and ZP3 to the vesicular aggregate and the close proximity of this structure to the oocyte surface further support a role for the vesicular aggregate as an intermediary in the secretory pathway of ZP glycoproteins. The enhanced staining property of the vesicular aggregate, as revealed by the use of ferrocyanide-reduced osmium, reflects the presence of carbohydrate moieties associated with newly synthesized macromolecules presumably coming from the Golgi complex. These results further support previous findings that the mouse ZP glycoproteins are synthesized and secreted by ovarian oocytes [30–32] and not by granulosa cells, which were devoid of any labeling in the present study.

The question of whether the ZP is structurally homogeneous throughout its width remains the subject of some disagreement [14, 15]. Several studies indicated that the ZP consists of randomly arranged fibrillogranular material that gives it an amorphous, spongelike appearance in the scan-

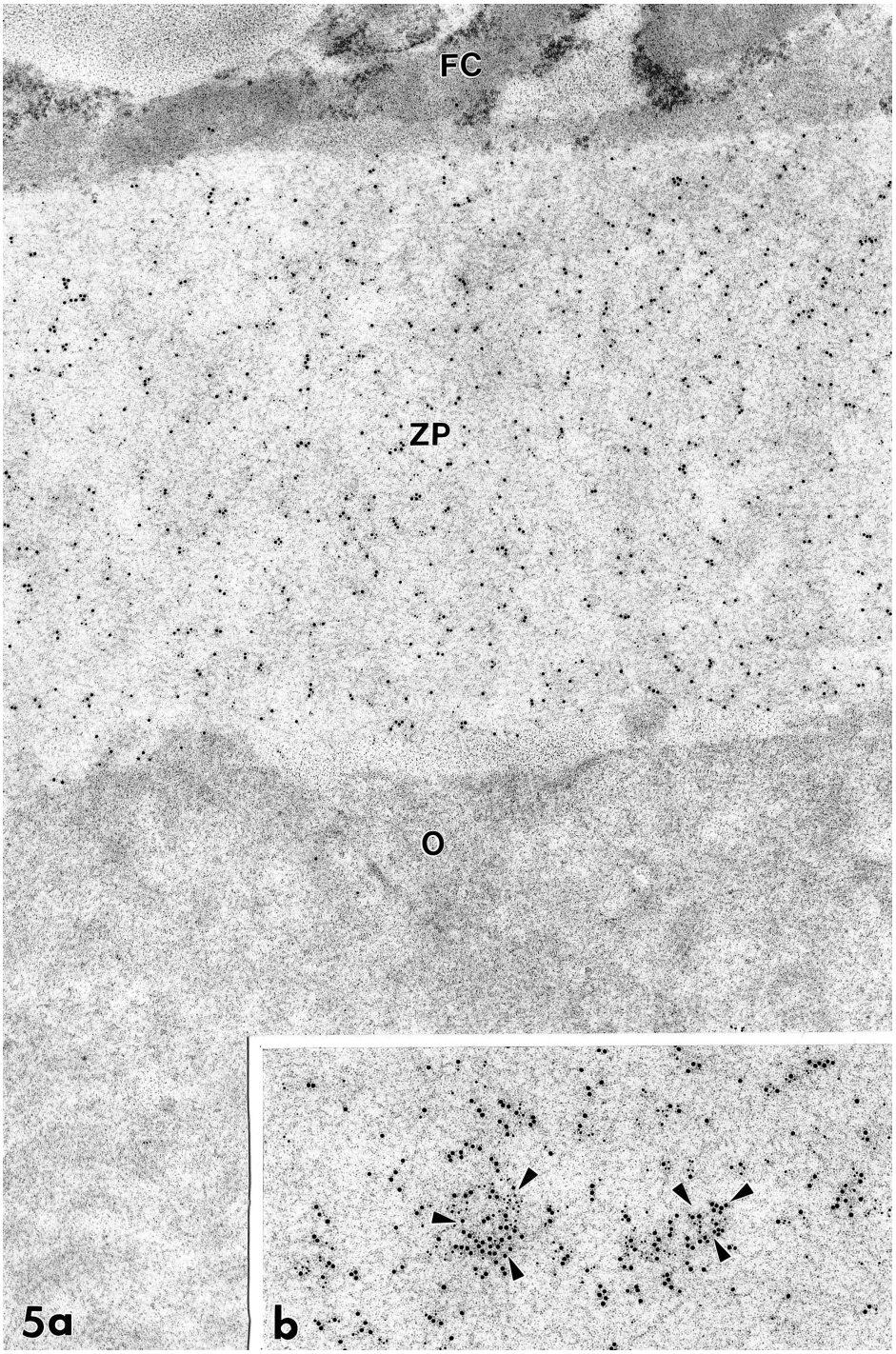

FIG. 5. An ovarian thin section labeled with a combination of anti-ZP1 antibody and anti-ZP3 antibody conjugated directly to 10-nm and 5-nm gold particles, respectively. **a**) At low magnification, a homogeneous distribution of the 10-nm and 5-nm gold particles is seen over the entire ZP. ×51 000. **b**) At high magnification, however, a close association between the 10-nm (representing ZP1) and 5-nm (representing ZP3) gold particles is common (arrowheads). The distance between many of the 10-nm gold particles (representing ZP1) is <10 nm. ×70 000. FC, Follicular cell; O, oocyte.

ning electron micrographs [33–35] and transmission electron micrographs [26, 36]. In a previous study in the hamster using the backscatterd electron imaging fracture label technique and lectin cytochemistry, the uniformity of the ZP was also demonstrated [37]. Results obtained in the present study using unconjugated and colloidal gold-conjugated antibodies directed against ZP1, ZP2, or ZP3 revealed a different pattern of distribution of gold particles over the ZP. When unconjugated rat anti-mouse ZP monoclonal antibodies were applied to ovarian sections at the electron microscope level, immunoreactivity to each of the ZP glycoproteins remained uniform throughout the entire width of the ZP irrespective of the developmental stage of the ovarian follicles. However, the use of specific antibodies tagged with gold particles of different sizes demonstrated an asymmetrical distribution of the different ZP glycoproteins in the zona matrix, with a higher concentration of gold labeling in the inner region. Also, there was a noticeable difference in the intensity of immunolabeling between the unconjugated rat IgG and the colloidal gold-conjugated antibodies for each of the ZP glycoproteins. Although we cannot explain the reason for the difference in the distribution and the intensity of the labeling, one possible explanation involves the steric interference factor presumably associated with each of the gold-conjugated antibodies during binding to their respective glycoproteins. Immunocytochemical results presented in this study revealed some unique structural aspects of the ZP regardless of which antibody set was

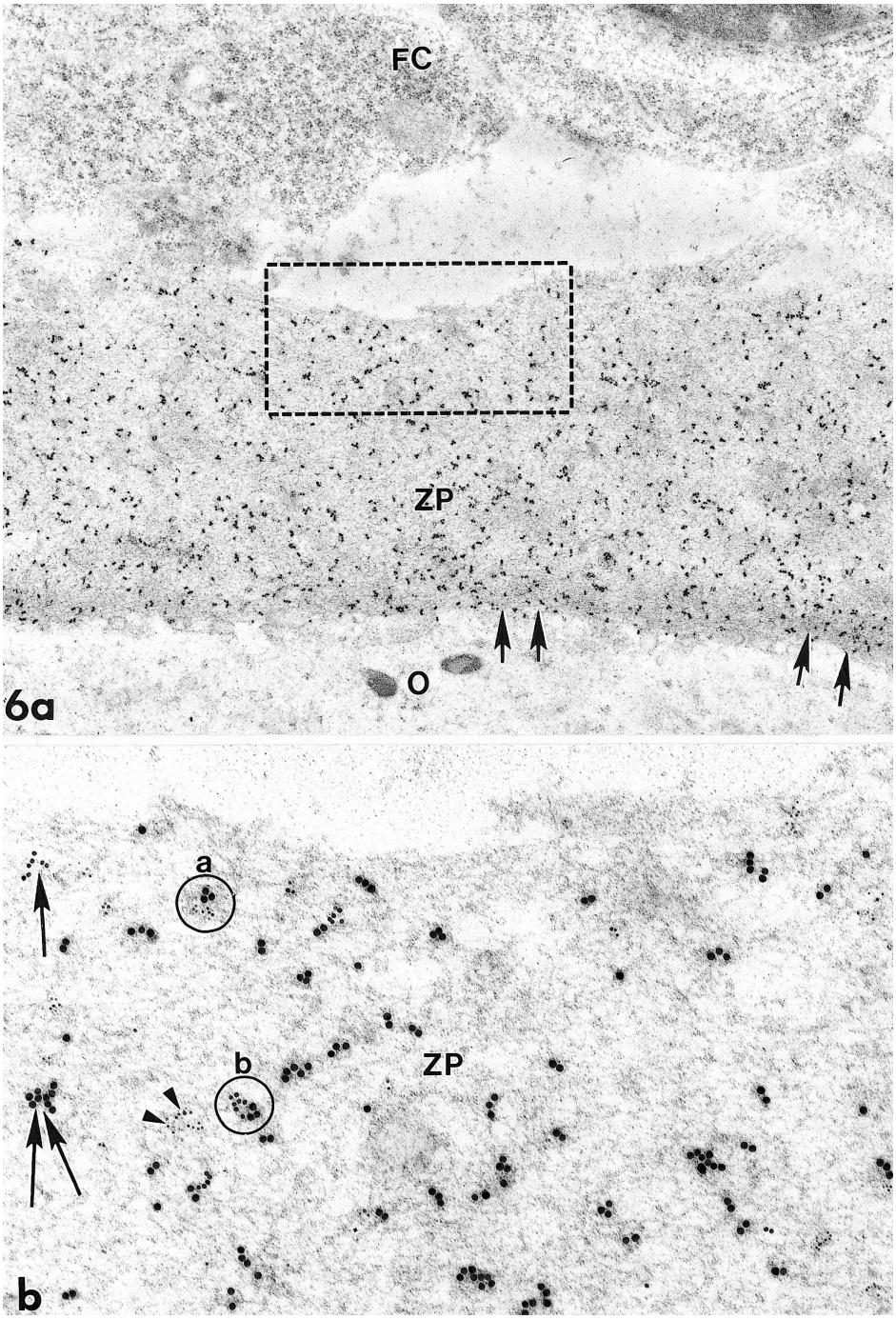

FIG. 6. Lowicryl section showing an ovarian oocyte labeled with a combination of anti-ZP1, anti-ZP2, and anti-ZP3 antibodies tagged directly to 15-nm, 10-nm, and 5-nm gold particles, respectively. **a**) At low magnification, labeling by the three antibodies occupies the entire ZP, with a relatively higher concentration of gold labeling detected in the inner layer of the ZP (arrows). Follicular cells (FC) are not labeled. ×21 000. **b**) A high magnification view of the area in the framed box reveals the distribution of gold labeling by the various antibody-gold conjugates in the outer layer of the ZP. Labeling by gold particles is often seen as clusters of 10-nm gold particles (arrow), 15-nm gold particles (double arrows), or 5-nm gold particles (arrowheads). Association between two particle sizes such as 15 and 5 nm (circle a) or 15 and 10 nm (circle b) is often seen. ×90 000.

used. Favorably cut Lowicryl-embedded ovarian tissue sections demonstrated an association of immunolabeling, most prominently by anti-ZP3 antibody, with horizontal arrays of filamentous material located in the outer layer of the ZP. Previously, the use of polarized light microscopy and digital image processing has shown that the hamster ZP is a multilaminar structure [38]. With this nondestructive method, the ZP filaments were shown to be oriented tangentially in the outer layer of the ZP and radially in the inner layer. In our study, favorably cut sections of mouse ovaries revealed immunogold particles (representing ZP3) directly superimposed on tangentially oriented linear arrays of filaments located in the outer layer of the mouse zona matrix. In the inner layer, gold particles were also associated specifically with linear arrays of filaments, many of which were oriented radially. We did not detect any difference between the inner and outer ZP in the pattern of labeling by either the unconjugated rat IgG or the gold-conjugated antibodies. Whether the current model depicting the structure of mammalian ZP [17] can be applied to both the outer and inner layers remains to be determined.

The current model of the ZP structure proposed by Wassarman and Mortillo [17] stipulates that the ZP matrix in the mouse is composed of a network of interconnecting filaments and that these filaments are polymers composed of ZP2-ZP3 heterodimers interconnected by ZP1, the least abundant glycoprotein. Although this model is consistent with previous ultrastructural, biochemical and gene knockout and antisense experiments [16, 39–41], the current structure of the ZP, as proposed by the Wassarman group,

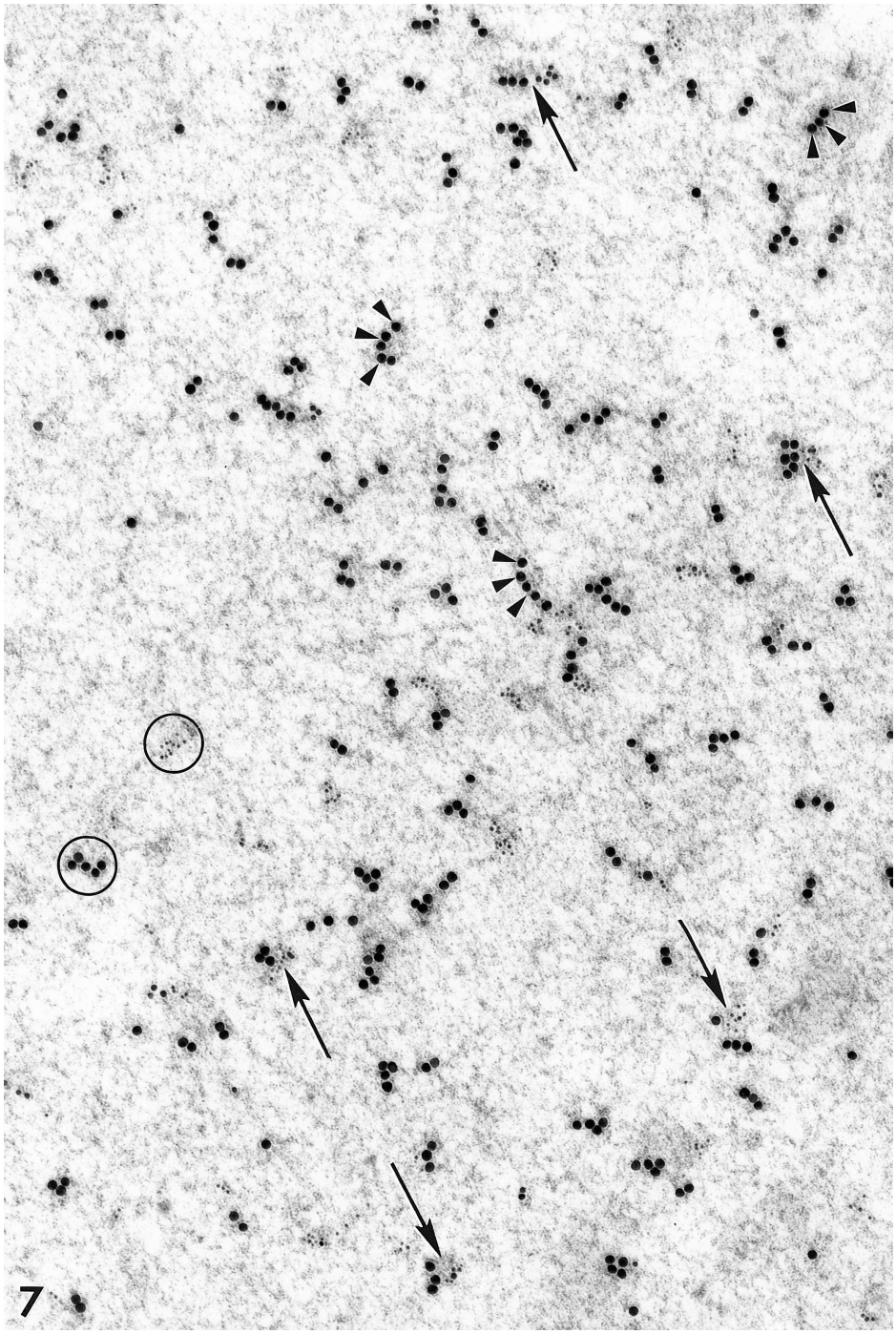

FIG. 7. A high magnification electron micrograph showing the ZP of an ovarian oocyte labeled with a mixture of anti-ZP1 antibody directly conjugated to 15-nm gold particles, anti-ZP2 antibody directly conjugated to 10-nm gold particles, and anti-ZP3 antibody directly conjugated to 5-nm gold particles. Most of the gold particles are located on dark patches of a filamentous nature (arrowheads), usually in clusters of one particular gold size (circles). In many of these dark filamentous patches, 10-nm gold particles (representing ZP2) and/or 5-nm gold particles (representing ZP3) are closely associated with 15-nm gold particles (representing ZP1). Where the 15-nm gold particles form linear arrays (arrowheads), the 15-nm gold particles (representing ZP1) are always less than 10 nm apart. ×120 000.

remains unproven. It is still not clear whether each monomer along a ZP filament, as stipulated in the current model, represents a single glycoprotein (ZP1, ZP2, or ZP3) or an oligomer consisting of two or more of the same or different glycoproteins. In the present study, when ovarian tissue sections were incubated with a combination of two or three antibody-gold solutions, there was a close association between 10-nm and 5-nm gold particles representing, respectively, ZP2 and ZP3, which might be explained by the heterodimeric nature of ZP2 and ZP3, as postulated by the Wassarman group.

One of the unanswered questions with regard to the current ZP model is whether ZP1 molecules cross-linking ZP filaments are located at regularly spaced intervals [16]. According to the Wassarman model, each ZP2-ZP3 unit has been estimated to be 15–17 nm in length (center to center distance) along the axis of ZP filaments, and for a ratio of ZP1:ZP2-ZP3 dimer of 1:5, the mean length between attachment sites on each filament is approximately 75–85 nm [42]. Both double and triple immunolocalization experiments revealed that ZP1 macromolecules (represented by 15-nm gold particles), confined to small patches of filamentous material, were often seen in close proximity to one another. The apparent distance separating the neighboring 15-nm gold particles along the axis of filamentous patches appeared always to be <10 nm. Therefore, the spacing of ZP1 dimers as cross-linking sites of the ZP2-ZP3 heterodimers may be much closer than that previously proposed [42]. As a result, the number of ZP1 dimers as anchoring sites could be larger than previously predicted.

Another observation made in the present study provides new information about the stoichiometric disposition of ZP1 in relation to ZP3. A high concentration of gold particles was always seen in the zona matrix when 10-nm gold-anti-ZP3 antibody conjugate was used alone. However, when a mixture of 15-nm (ZP1) and 10-nm (ZP3) gold particles was used for labeling the ovarian sections, despite the larger 15-nm gold particles that normally cause steric hindrance, there appeared to be a stronger labeling for ZP1 than for ZP3. This difference might be due to the unique stoichiometric disposition of ZP1 in the zona matrix, rendering the ZP1 antigenic sites more accessible to labeling by the 15-nm gold-conjugated antibody. ZP3 is likely to be very close to ZP1 and, thus, partially masked by ZP1, resulting in a lower intensity of labeling for ZP3 when used in conjunction with anti-ZP1 antibody-gold (15 nm) conjugate. Despite the size of the 15-nm gold particles, the anti-ZP1 antibody may have easier access to the larger and presumably more exposed ZP1 dimer, with a molecular mass of 200 000. As a result, anti-ZP1 antibody-colloidal gold particles are bound first to the corresponding antigenic sites, creating a steric hindrance for the 10-nm gold-anti-ZP3 antibody conjugate to reach the partially masked ZP3 macromolecules, in particular those that are in the immediate vicinity of the ZP1 dimers. Therefore, it is quite possible that within the three-dimensional zona matrix, ZP1 dimers are more likely to cross-link to the ZP3 molecule(s) located along the axis of one ZP filament than to the ZP3 molecule(s) located in another heterodimeric filament.

Three important results were obtained using specific antibodies against the major mouse ZP glycoproteins. First, the vesicular aggregate, a complex of vesicles previously reported in the oocyte proper of several mammalian species including humans, is likely to be involved in the processing and secretion of ZP1, ZP2, and ZP3. Second, the association of gold/immunogold labeling with both tangential and radial arrays of filaments, characterizing the inner and the outer zone of the ZP, respectively, as previously reported in the hamster, provides further insight into the biochemical nature of these filaments. Third, the patterns of immunolabeling generated by the anti-ZP1 antibody suggest that the disposition and the ratio of ZP1 macromolecules cross-linking the various ZP filaments may differ from those previously predicted. These results lend support to the current model of ZP structure and provide additional information regarding the intracellular localization of the various ZP glycoproteins and their spatial topography within the three-dimensional structure of the zona pellucida.

ACKNOWLEDGMENTS

The authors thank Ms. Verna Norkum for technical assistance and Mr. Bob Temkin for reproduction of the original photomicrographs.

REFERENCES

1. Wassarman PM. Early events in mammalian fertilization. Annu Rev Cell Biol 1987; 3:109–142.
2. Yanagimachi R. Mammalian fertilization. In: Knobil E, Neil JD (eds.), The Physiology of Reproduction. New York: Raven Press; 1994: 189–317.
3. Greve JM, Salzmann GS, Roller RJ, Wassarman PM. Biosynthesis of the major zona pellucida glycoproteins secreted by oocytes during mammalian oogenesis. Cell 1982; 31:749–759.
4. Wolgemuth DJ, Celenza J, Bundman DS, Dunbar BS. Formation of the rabbit zona pellucida and its relationship to ovarian follicular development. Dev Biol 1984; 106:1–14.
5. Takeuchi IK, Takeuchi YK. Use of tannic acid for ultrastructural visualization of zonae pellucidae in growing oocytes in rat ovarian follicles. Zool Sci 1985; 2:135–139.
6. Tesarik J, Kopecny V. Late preovulatory synthesis of proteoglycans by the human oocyte and cumulus cells and their secretion into the oocyte-cumulus-complex extracellular matrices. Histochemistry 1986; 85:523–538.
7. Leveille MC, Roberts KD, Chevalier S, Chapdelaine A, Bleau G. Formation of the hamster zona pellucida in relation to ovarian differentiation and follicular growth. J Reprod Fertil 1987; 79:173–183.
8. Dunbar BS, Maresh GA, Washenik K. Ovarian development and the formation of the mammalian zona pellucida. In: Dietl J (ed.), The Mammalian Egg Coat. Structure and Function. Berlin: Springer-Verlag; 1989: 38–48.
9. Lee VH, Dunbar BS. Developmental expression of the rabbit 55-kDa zona pellucida protein and messenger RNA in ovarian follicles. Dev Biol 1993; 155:371–382.
10. Bleil JD, Wassarman PM. Synthesis of zona pellucida proteins by denuded and follicle-enclosed mouse oocytes during culture in vitro. Proc Natl Acad Sci U S A 1980; 77:1029–1033.
11. Shimizu S, Tsuji M, Dean J. In vitro biosynthesis of three sulfated glycoproteins of murine zonae pellucidae by oocytes grown in culture. J Biol Chem 1983; 258:5858–5863.
12. Wassarman PM. Profile of a mammalian sperm receptor. Development 1990; 108:1–17.
13. Wassarman PM. Regulation of mammalian fertilization by zona pellucida glycoproteins. J Reprod Fertil Suppl 1990; 42:79–87.
14. Dunbar BS, Wolgemuth DJ. Structure and function of the mammalian zona pellucida, a unique extracellular matrix. In: Satir BH (ed.), Modern Cell Biology, vol. 3. New York: Alan R. Liss; 1984: 77–111.
15. Wassarman PM. Zona pellucida glycoproteins. Annu Rev Biochem 1988; 57:415–442.
16. Greve JM, Wassarman PM. Mouse egg extracellular coat is a matrix of interconnected filaments possessing a structural repeat. J Mol Biol 1985; 181:253–264.
17. Wassarman PM, Mortillo S. Structure of the mouse egg extracellular coat, the zona pellucida. Int Rev Cytol 1990; 130:85–110.
18. Bleil JD, Wassarman PM. Structure and function of the zona pellucida: identification and characterization of the proteins of the mouse oocyte's zona pellucida. Dev Biol 1980; 76:185–202.
19. Karnovsky MJ. Use of ferrocyanide-reduced osmium tetroxide in electron microscopy. In: Program of the 11th annual meeting of the American Society of Cell Biology; New Orleans, LA; 1971. Abstract 284: 146.
20. East IJ, Dean J. Monoclonal antibodies as probes of the distribution of ZP2, the major sulfated glycoprotein of the murine zona pellucida. J Cell Biol 1984; 98:795–800.
21. East IJ, Gulyas BJ, Dean J. Monoclonal antibodies to murine zona pellucida protein with sperm receptor activity: effects on fertilization and early development. Dev Biol 1985; 109:268–273.
22. Rankin T, Talbot P, Lee E, Dean J. Abnormal zona pellucidae in mice lacking ZP1 result in early embryonic loss. Development 1999; 126: 3847–3855.
23. St-Jacques S, Bleau G. Monoclonal antibodies specific for an oviductal component associated with the hamster zona pellucida. J Reprod Immunol 1988; 12:247–261.
24. Wassarman PM. The mammalian ovum. In: Knobil E, Neill JD (eds.), The Physiology of Reproduction. New York: Raven Press; 1988: 69–134.
25. Merchant H, Chang MC. An electron microscopic study of mouse eggs matured in vivo and in vitro. Anat Rec 1971; 171:21–37.
26. Wassarman PM, Josefowicz WJ. Oocyte development in the mouse: an ultrastructural comparison of oocytes isolated at various stages of growth and meiotic competence. J Morphol 1978; 156:209–236.
27. Dvorak M, Sedlackova M. Ultrastructure and morphometric analysis of cytoplasmic structures in the mouse oocyte with germinal vesicles, oocyte at metaphase I and oocyte at metaphase II. Scr Med 1988; 61: 451–464.
28. Sathananthan AH. Ultrastructural changes during meiotic maturation in mammalian oocytes: unique aspects of the human oocyte. Microsc Res Tech 1994; 27:145–164.
29. Aviles M, El-Mestrah M, Jaber L, Castells MT, Ballesta J, Kan FWK. Cytochemical demonstration of modification of carbohydrates in the mouse zona pellucida during folliculogenesis. Histochem Cell Biol 2000; 113:207–219.
30. Roller RJ, Kinloch RA, Hiraoka Y, Li SSL, Wassarman PM. Gene expression during mammalian oogenesis and early embryogenesis:

quantification of three messenger RNAs abundant in fully grown mouse. Development 1989; 106:251–261.
31. Kinloch RA, Wassarman PM. Profile of a mammalian sperm receptor gene. New Biol 1989; 1:232–238.
32. Liang LF, Chamow SM, Dean J. Oocyte-specific expression of mouse ZP2: developmental regulation of the zona pellucida genes. Mol Cell Biol 1990; 10:1507–1515.
33. Philips DM, Shalgi RM. Surface properties of the zona pellucida. J Exp Zool 1980; 213:1–8.
34. Philips DM, Shalgi R, Dekel N. Mammalian fertilization as seen with the scanning electron microscope. Am J Anat 1985; 174:357–372.
35. Familiari G, Nottola SA, Macchiarelli G, Micara G, Aragona C, Motta PM. Human zona pellucida during in vitro fertilization: an ultrastructural study using saponin, ruthenium red and osmium thiocarbohydrazide. Mol Reprod Dev 1992; 32:51–61.
36. Dietl J, Czuppon AB. Ultrastructural studies of the porcine zona pellucida during the solubilization process by Li-3.5-diodosalicylate. Gamete Res 1984; 9:45–54
37. Kan FWK, Zalzal S, Roux E, Nanci A. Homogeneity in the distribution of matrix components in the hamster zona pellucida as revealed by backscattered electron imaging fracture-label. Anat Rec 1994; 239: 35–46.
38. Keefe D, Tran P, Pellegrini C, Oldenbourg R. Polarized light microscopy and digital image processing identify a multilaminar structure of the hamster zona pellucida. Hum Reprod 1997; 12:1250–1252.
39. Epifano O, Liang LF, Familiari M, Moos MC, Dean J. Coordinate expression of the three zona pellucida genes during mouse oogenesis. Development 1995; 121:1947–1956.
40. Liu C, Litscher ES, Mortillo S, Sakai Y, Kinloch RA, Stewart CI, Wassarman PM. Targeted disruption of the mZP3 gene results in production of eggs lacking a zona pellucida and infertility in female mice. Proc Natl Acad Sci U S A 1996; 93:5431–5436.
41. Rankin T, Familiari M, Lee E, Ginsberg A, Dwyer N, Blanchette-Mackie J, Drago J, Westphal H, Dean J. Mice homozygous for an insertional mutation in the ZP3 gene lack a zona pellucida and are infertile. Development 1996; 122:2903–2910.
42. Green D. Three-dimensional structure of the zona pellucida. Rev Reprod 1997; 2:147–156.